

---

# SupertonicTTS: Towards Highly Scalable and Efficient Text-to-Speech System

---

**Hyeongju Kim**  
Supertone, Inc.  
hyeongju@supertone.ai

**Jinhyeok Yang**  
Supertone, Inc.  
yangyangii@supertone.ai

**Yechan Yu**  
Supertone, Inc.  
ato@supertone.ai

**Seunghun Ji**  
Supertone, Inc.  
allay@supertone.ai

**Jacob Morton**  
Supertone, Inc.  
jake@supertone.ai

**Frederik Bous**  
Supertone, Inc.  
bous@supertone.ai

**Joon Byun**  
Supertone, Inc.  
joonbyun@supertone.ai

**Juheon Lee**  
Supertone, Inc.  
juheon@supertone.ai

## Abstract

We present a novel text-to-speech (TTS) system, namely SupertonicTTS, for improved scalability and efficiency in speech synthesis. SupertonicTTS is comprised of three components: a speech autoencoder for continuous latent representation, a text-to-latent module leveraging flow-matching for text-to-latent mapping, and an utterance-level duration predictor. To enable a lightweight architecture, we employ a low-dimensional latent space, temporal compression of latents, and ConvNeXt blocks. We further simplify the TTS pipeline by operating directly on raw character-level text and employing cross-attention for text-speech alignment, thus eliminating the need for grapheme-to-phoneme (G2P) modules and external aligners. In addition, we introduce context-sharing batch expansion that accelerates loss convergence and stabilizes text-speech alignment. Experimental results demonstrate that SupertonicTTS achieves competitive performance while significantly reducing architectural complexity and computational overhead compared to contemporary TTS models. Audio samples demonstrating the capabilities of SupertonicTTS are available at: <https://supertoniccts.github.io/>.

## 1 Introduction

Text-to-speech (TTS) technology has made remarkable advancements in recent years, unlocking groundbreaking capabilities and enhancing user experiences. For instance, modern TTS models can synthesize natural voice for speakers unseen during training [5, 20, 46]. This is achieved with only a few adaptation steps using a small amount of data [16, 27] or even without any fine-tuning at all, a feature referred to as zero-shot capability [5, 20, 25]. Moreover, modern TTS systems provide a wide range of powerful functionalities within a single model, such as voice conversion [24, 5], multilingual synthesis [6, 25], content editing [49, 41], and noise removal [30].

To achieve these breakthroughs, researchers have explored diverse approaches to TTS modeling. One prominent direction involves using signal processing features, such as mel spectrograms, as intermediate representations [19, 23, 29, 10]. This approach typically employs two separate models: one to convert text into signal processing features and another to generate a waveform from these features. Another common approach is to leverage discrete tokens derived from neural codec models

Table 1: Comparison of SupertonicTTS with recent text-to-speech models (“Phn. Dur.”: phoneme-level duration requirement, “TS Aligner”: use of text-to-speech aligner during training, “Ref. Text”: reference speech transcription requirement, “TP”: text processor, “SR”: sampling rate, “#Param.”: total parameter count including duration predictor and vocoder). † indicates that the number is an estimate based on architecture descriptions in the baseline papers.

	Phn. Dur.	TS Aligner	Ref. Text	TP	SR (Hz)	#Param.
VALL-E [51]	✗	✗	✓	G2P	24,000	410M <sup>†</sup>
VoiceBox [30]	✓	✓	✓	G2P	16,000	371M
Mega-TTS 2 [20]	✓	✓	✗	G2P	16,000	473M
CLaM-TTS [25]	✗	✗	✓	ByT5 [53]	22,050	>1.3B <sup>†</sup>
DiTTo-TTS [31]	✗	✗	✓	SpeechT5 [1]	22,050	970M
SupertonicTTS	✗	✗	✗	<b>raw</b>	<b>44,100</b>	<b>44M</b>

as intermediate representations [22, 25, 51]. The discrete nature of these features enables language modeling, resulting in improved naturalness, intelligibility, and speaker similarity. Furthermore, disentangled latent spaces are often used to provide control over speech features such as pitch, content, and timbre [21, 8].

Despite significant technical achievements, however, most contemporary TTS systems still require a large number of parameters, massive speech-text training data, and a complex pipeline that includes a grapheme-to-phoneme (G2P) module, a text-speech aligner, or pretrained models for extracting textual and speaker features, as outlined in Table 1. These factors collectively contribute to increased computational overhead during training and inference, and introduce complex interdependencies among system components. Given these challenges, a promising research direction in TTS is to develop a more streamlined pipeline that reduces architectural complexity and training overhead while maintaining competitive performance. The approach of this paper seeks to improve both efficiency and scalability, in line with recent trends in large language models (LLMs) that focus on cost-effective training and optimized inference [33, 9].

To address these challenges effectively while ensuring competitive performance, we propose a novel TTS system, namely **SupertonicTTS**. This system consists of three modules: (1) **a speech autoencoder** that encodes audio into a continuous latent representation, (2) **a text-to-latent module** that maps text and speaker information to corresponding latents using a flow-matching algorithm [32], and (3) **a duration predictor** that estimates the total duration of speech to be synthesized. Specifically, the speech autoencoder is trained to compress audio into a latent space and accurately reconstruct it. The text-to-latent module learns to estimate a conditional probability path to generate latents from noise given text and reference speech. Unlike conventional phoneme-level duration models, the duration predictor is optimized to estimate the total speech duration. During inference, the text-to-latent module generates latents with the predicted utterance duration based on input text and reference speech, which are then decoded by the speech autoencoder to produce 44.1 kHz audio. Our approach is based on recent advancements in generative models, particularly latent diffusion models (LDMs) [43, 45, 36, 37].

We introduce several techniques to significantly enhance scalability and efficiency. First, we design the latent space with a remarkably low dimensionality and compress the latents along the temporal axis before passing them to the text-to-latent module. This strategy significantly reduces the computational overhead of subsequent processes. Second, we introduce context-sharing batch expansion to accelerate loss convergence, offering benefits similar to increasing batch size, but with comparatively lower computational cost. We provide empirical evidence that the proposed batch expansion effectively facilitates accurate text-speech alignment learning. Third, we employ ConvNeXt blocks [34, 47, 39] extensively across all modules to ensure a lightweight and efficient architecture. In addition to these primary contributions, we simplify the TTS pipeline by employing cross-attention mechanisms for text-speech alignment, similar to [31, 37], and by using raw character-level text as input. This design choice removes the need for an external aligner and a grapheme-to-phoneme (G2P) model, which can often become bottlenecks when scaling to new data domains or languages. Furthermore, we refrain from incorporating external pretrained models, thereby reducing architectural dependencies and complexity. Table 1 provides a comprehensive comparison of the proposed system against other TTS models.

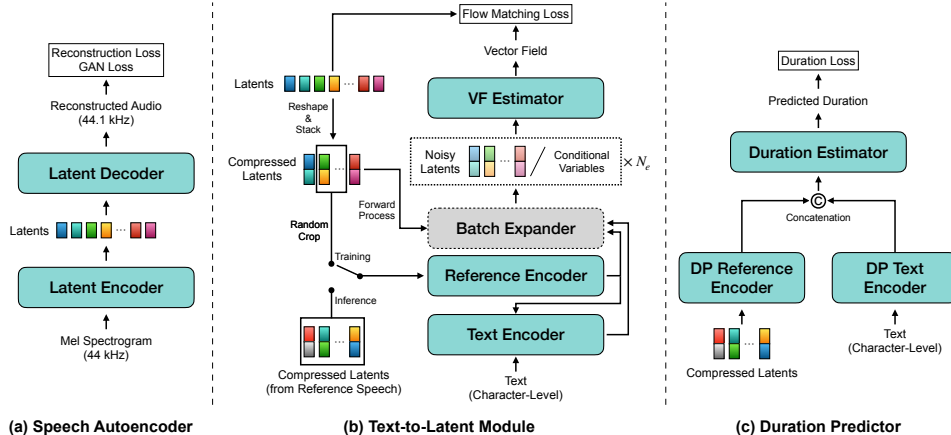


Figure 1: Overall architecture of SupertonicTTS.

Through extensive experimentation, we rigorously evaluate SupertonicTTS and confirm its key contributions. First, we demonstrate its ability to reconstruct high-fidelity speech from compressed latent representations with remarkably fast inference. Second, we show that context-sharing batch expansion accelerates both loss convergence and text-speech alignment learning, offering memory and computational efficiency. Finally, we demonstrate that SupertonicTTS achieves competitive zero-shot TTS performance with just 44 million parameters and extremely fast generation. Audio samples are available at <https://supertonicetts.github.io/>.

## 2 Method

SupertonicTTS is built around latent diffusion, which has shown state-of-the-art performance in different generative tasks [45, 36, 43]. More specifically, the training of SupertonicTTS is divided into three phases: first, a speech autoencoder is trained to map input audio into a low-dimensional latent space and reconstruct the original audio. Next, a text-to-latent module learns to generate latent representations that accurately reflect the speech characteristics of both input text and reference speech. Finally, a duration predictor is optimized to estimate the total speech duration based on input text and reference speech.

To ensure fast inference and architectural efficiency, SupertonicTTS primarily employs ConvNeXt blocks [34], which have recently shown competitive performance in speech generation [39, 47, 52]. The entire pipeline is further streamlined by excluding external pretrained models, text-speech aligners, and G2P modules. The overall architecture of SupertonicTTS is depicted in Figure 1 and detailed descriptions of each component are provided in the following sections.

### 2.1 Speech autoencoder

The speech autoencoder converts input audio into latent representations using a latent encoder and reconstructs the audio from these representations with a latent decoder. In this work, we use the mel spectrogram as the input features to the latent encoder instead of raw audio. Our preliminary experiments show that this approach accelerates the convergence of the training loss compared to using raw audio input. The latent space is designed to be continuous and **significantly lower in dimensionality** than the number of mel spectrogram channels. The input-output structure of the speech autoencoder aligns with that of conventional neural vocoders. Therefore, the speech autoencoder can be interpreted as a neural vocoder with a compact latent space in its middle.

#### 2.1.1 Architecture

The latent encoder is built upon the Vocos architecture, which is primarily composed of ConvNeXt blocks for improved computational efficiency [47, 34]. To tailor the architecture for latent encoding, we remove the original Fourier head and introduce a linear layer just before the final normalization. This linear layer projects hidden representations into a lower-dimensional space. Although the

latent encoder is not used during TTS inference, its efficient design is leveraged to enable fast latent encoding throughout the training of the text-to-latent module.

Similarly, the latent decoder follows the Vocos architecture with several key modifications. First, we adapt a depth-wise convolution layer in the ConvNeXt blocks to be causal and dilated. The introduction of causal layers allows the latent decoder to operate in streaming mode. Additionally, instead of using the Fourier head, we introduce two linear layers with PReLU activation [12]. The final time-domain output is derived by flattening the frame-level output. This approach is inspired by WaveNeXt [39], but we adopt a higher hidden dimensionality with nonlinearity to enhance representational capacity. Architectural details are provided in Appendix A.1.

### 2.1.2 Optimization

Similar to modern neural vocoders [10, 29], the speech autoencoder is trained within a Generative Adversarial Network (GAN) framework [11], using a combination of reconstruction loss  $\mathcal{L}_{\text{recon}}$ , adversarial loss  $\mathcal{L}_{\text{adv}}$ , and feature matching loss  $\mathcal{L}_{\text{fm}}$ . The reconstruction loss is defined as the multi-resolution spectral  $L_1$  loss, computed in the mel spectrogram domain. For adversarial training, both multi-period discriminators (MPD) [29] and multi-resolution discriminators (MRD) [18] are employed to enhance perceptual quality. Additionally, the feature matching loss is applied to minimize the  $L_1$  distances between the discriminator features of real and generated samples, thereby further stabilizing the adversarial training process. The final loss for the training phase of generator is given by  $\mathcal{L}_G = \lambda_{\text{recon}}\mathcal{L}_{\text{recon}} + \lambda_{\text{adv}}\mathcal{L}_{\text{adv}} + \lambda_{\text{fm}}\mathcal{L}_{\text{fm}}$ . Further details on the discriminator architecture and objective functions can be found in Appendices A.1.3 and B.1.

## 2.2 Text-to-latent module

The text-to-latent module generates a latent representation that captures essential speech characteristics from both input text and reference speech, following the LDM framework [36, 43, 45]. Specifically, an initial noise  $z_0$  is drawn from a base distribution  $p(z_0)$ , typically set as a simple prior such as  $\mathcal{N}(0, I)$ . The noise is then progressively refined into a structured representation  $z_t$  through a time-dependent vector field induced by the flow-matching framework [32]. The text-to-latent module estimates this vector field based on text, reference speech, and time  $t$ , ensuring that the final representation  $z_1$  preserves the relevant speech attributes.

Unlike most recent state-of-the-art TTS models, the text-to-latent module **does not rely on external pretrained models, G2P modules, or text-to-speech aligners**. Specifically, it uses character-level text as input and employs cross-attention mechanisms to align text and speech within a streamlined architecture. To improve training efficiency and convergence, we also introduce two novel techniques: **temporal compression of latents** and **context-sharing batch expansion**.

### 2.2.1 Temporally compressed latent representation

We propose modeling temporally compressed latents that are reshaped and stacked along the channel dimension. Specifically, for a given compression factor  $K_c$ , the latent shape is transformed from  $(C, T)$  to  $(C \times K_c, \frac{T}{K_c})$ , where  $C$  represents the original latent dimensionality and  $T$  denotes the number of temporal frames. To this end, we set the original latent dimensionality to a relatively low value, thereby ensuring that the compressed latents maintain a moderate level of dimensionality (e.g.,  $C \times K_c = 144$ ). This approach provides several advantages over using the original latents. First, it alleviates the text-speech alignment challenge by reducing the total number of speech frames. Second, it reduces computational costs, which is particularly advantageous for layers that rely on computationally intensive sequential operations such as the attention mechanism [50]. Finally, all temporal information is preserved in the transformed representation, allowing for perfect reconstruction by simply reversing the compression process.

### 2.2.2 Context-sharing batch expansion for efficient training

We introduce context-sharing batch expansion to improve the training efficiency of conditional generative models that are based on diffusion or flow-matching algorithms [14, 48, 32]. In conventional training setups, these generative algorithms sample noise and a diffusion timestep to perturb an input variable (forward process) and optimize the models to denoise it using the provided conditional

---

**Algorithm 1** Training with Context-Sharing Batch Expansion

---

**Require:** Diffusion model  $f_\theta$ , condition encoder  $g_\phi$ , mini-batch  $\{(x_i, c_i)\}_{i=1}^B$ , expansion factor  $K_e$

- 1: Encode the conditional variables:  $\{\bar{c}_i\}_{i=1}^B \leftarrow g_\phi(\{c_i\}_{i=1}^B)$
- 2: Initialize expanded batch  $\mathcal{B}_{\text{exp}} \leftarrow \emptyset$
- 3: **for**  $i = 1$  to  $B$  **do**
- 4:     **for**  $k = 1$  to  $K_e$  **do**
- 5:         Sample noise  $\epsilon_i^k$ , timestep  $t_i^k$
- 6:          $\tilde{x}_i^k \leftarrow \text{ForwardProcess}(x_i, \epsilon_i^k, t_i^k)$
- 7:         Append  $(\tilde{x}_i^k, \bar{c}_i, t_i^k)$  to  $\mathcal{B}_{\text{exp}}$       $\triangleright$  Encoded condition  $\bar{c}_i$  is shared across  $K_e$  samples
- 8:     **end for**
- 9: **end for**
- 10: Optimize  $f_\theta$  using  $\mathcal{B}_{\text{exp}}$

---

variables (reverse process). In contrast, the proposed batch expansion samples multiple noise instances to produce several perturbed input variables at different diffusion timesteps. Meanwhile, the corresponding conditional variables are reused by duplication<sup>1</sup>. This strategy mimics the effect of increasing batch size but is computationally more efficient because conditional variables are shared across multiple perturbed inputs (i.e., context-sharing). A pseudo-algorithm is provided in Algorithm 1 for further clarification.

### 2.2.3 Architecture

The reference encoder takes temporally compressed latents as input. These latents are obtained by cropping a portion of the training data during training, and extracted from reference speech during inference. It then processes the latents using multiple ConvNeXt blocks and generates reference key and value representations through two attention layers, similar to the timbre token block in NANSY++ [8]. Note that the reference key and value are fixed-size vectors, independent of the input length.

The text encoder processes character-level input using ConvNeXt blocks and self-attention layers. This architecture is designed to efficiently capture both local and long-range dependencies in text, offering computational efficiency. The output from the self-attention layers is further refined using reference key and value vectors through two cross-attention layers, producing speaker-adaptive text representations.

The vector field (VF) estimator is mainly composed of ConvNeXt blocks, along with time-conditioning, text-conditioning, and reference-conditioning blocks. To enhance model expressiveness, certain ConvNeXt blocks incorporate dilated convolutional layers. Time conditioning is achieved by globally adding a time embedding to the input sequence. Both text and reference conditioning utilize cross-attention, where the conditional variables serve as keys and values. More details on the architecture of the text-to-latent module can be found in Appendix A.2.

### 2.2.4 Optimization

The text-to-latent module is optimized using the flow-matching algorithm [32]. During training, a randomly cropped segment of the compressed latents serves as input to the reference encoder. To prevent information leakage from this, we apply a mask to the corresponding segment when calculating the flow-matching loss, similar to previous work [31, 28]. Specifically, our optimization objective is as follows:

$$\mathcal{L}_{\text{TTL}} = \mathbb{E}_{t, (z_1, c), p(z_0)} \|\mathbf{m} \cdot (v(z_t, z_{\text{ref}}, c, t) - (z_1 - (1 - \sigma_{\text{min}})z_0))\|_1, \quad (1)$$

where  $v$ ,  $\mathbf{m}$ ,  $z_1$ ,  $z_0$ ,  $z_t$ ,  $z_{\text{ref}}$ , and  $c$  represent the text-to-latent module, the reference mask, compressed latents, noise sampled from the base distribution  $p(z_0)$ , noisy latents  $z_t = (1 - (1 - \sigma_{\text{min}})t)z_0 + z_1$ , cropped latents  $z_{\text{ref}} = (1 - \mathbf{m}) \cdot z_1$ , and text, respectively. We set  $t \sim \mathcal{U}[0, 1]$  and  $p(z_0) = \mathcal{N}(0, 1)$ . Furthermore, with a probability of  $p_{\text{uncond}}$ , the model is trained without conditional variables  $z_{\text{ref}}$  and  $c$  to enable classifier-free guidance (CFG) [13]. In this case, the conditional inputs to the VF estimator, derived from text and reference speech, are replaced with learnable parameters.

---

<sup>1</sup>We assume that the conditional variables are already encoded by individual neural networks.

## 2.3 Duration predictor

At inference time, the proposed framework requires *the total length* of latent representations to be synthesized. In this context, SupertonicTTS is expected to be robust to errors in duration estimation, compared to other TTS models that rely on *phoneme-level* duration information [24, 28, 30, 55]. With this in mind, we design **an utterance-level duration predictor** with a simple yet effective architecture. Specifically, an utterance-level text embedding and a reference embedding are extracted from the text input and reference speech, respectively, using ConvNext blocks and attention layers. These embeddings are concatenated and transformed into a scalar value representing the total speech duration via linear layers. The duration predictor is trained using the  $L_1$  distance between the ground truth and predicted durations. Further details are provided in Appendix A.3.

## 3 Training setup

### 3.1 Dataset

To train the speech autoencoder, we combined publicly available datasets with our internal database, resulting in a total of 11,167 hours of audio recordings from approximately 14,000 speakers. For the training of the text-to-latent module and the duration predictor, we selected four English datasets: LJSpeech [17], VCTK [54], Hi-Fi TTS [3], and LibriTTS [56]. Collectively, these datasets encompass 945 hours of high-quality speech from 2,576 English speakers. All audio files were resampled to a target sample rate of 44.1 kHz, if their original sample rate differed.

### 3.2 Optimization

We optimized the speech autoencoder for 1.5M iterations using the AdamW optimizer [35] with a learning rate of  $2 \times 10^{-4}$  and a batch size of 128. We used four NVIDIA RTX 4090 GPUs. The loss function coefficients for training the generator were configured as follows:  $\mathcal{L}_{\text{recon}} = 45$ ,  $\mathcal{L}_{\text{adv}} = 1$ , and  $\mathcal{L}_{\text{fm}} = 0.1$ . For adversarial training, we randomly cropped segments of real and generated speech to 0.19 s, following the approach in VITS [24]. The log-scaled mel spectrogram input was obtained using an FFT size of 2048 (46.43 ms), a Hann window of the same size, a hop size of 512 (11.61 ms), and 228 mel bands. The dimension of the latent space was set to 24, approximately one-tenth of the input mel spectrogram channels. Additional details on the optimization of the speech autoencoder are provided in Appendix B.1.

The text-to-latent module was optimized using the AdamW optimizer for 700k iterations with a batch size of 64 and an expansion factor  $K_e = 4$ . The learning rate was initially set to  $5 \times 10^{-4}$  and reduced by half every 300k iterations. Training was conducted on four RTX 4090 GPUs. Latents were normalized using precomputed channel-wise mean and variance statistics before being input into the text-to-latent module. The temporal compression factor  $K_c$  was set to 6, resulting in a compressed latent dimension of 144. We set  $p_{\text{uncond}} = 0.05$  and  $\sigma_{\text{min}} = 10^{-8}$ . During training, reference speech segments were obtained by randomly cropping the input audio, with durations ranging from 0.2 s to 9 s. We ensured that the cropped length did not exceed half of the original speech duration.

The duration predictor was trained for 3,000 iterations using the AdamW optimizer with a learning rate of  $5 \times 10^{-4}$  and a batch size of 128 on a single RTX 4090 GPU. During training, reference speech was obtained by randomly selecting a segment from 5% to 95% of the input speech.

## 4 Experiments

### 4.1 Speech reconstruction

For evaluation of speech reconstruction, we compare the speech autoencoder with BigVGAN<sup>2</sup> [10], a state-of-the-art vocoder, using NISQA [38], UTMOSv2 [2], and CREPE [26]. Both NISQA and UTMOSv2 are non-intrusive mean opinion score (MOS) prediction systems to evaluate the perceptual quality of speech signals. Meanwhile, we use CREPE to analyze pitch in speech and compute the F1 score for voiced/unvoiced classification (V/UV F1), which serves as a key metric for identifying

<sup>2</sup>We use the official 44.1 kHz BigVGAN-v2 checkpoint, pretrained on multilingual speech, environmental sounds, and musical instruments.

Table 2: Evaluation of speech reconstruction on LibriTTS testsets with real-time factor (RTF).

	test-clean			test-other			RTF
	NISQA	UTMOSv2	V/UV F1	NISQA	UTMOSv2	V/UV F1	
GT	4.09 $\pm$ 0.03	<b>3.26</b> $\pm$ 0.02	-	3.61 $\pm$ 0.03	<b>3.01</b> $\pm$ 0.02	-	-
BigVGAN	<b>4.11</b> $\pm$ 0.03	3.16 $\pm$ 0.02	<b>0.9735</b>	3.61 $\pm$ 0.03	2.85 $\pm$ 0.02	<b>0.9620</b>	0.0124
Ours	4.06 $\pm$ 0.03	3.13 $\pm$ 0.02	0.9587	<b>3.76</b> $\pm$ 0.03	2.88 $\pm$ 0.02	0.9450	<b>0.0006</b>

Table 3: Performance comparison across different numbers of function evaluations. Best results are highlighted in bold, and second-best are underlined.

	NFE	RTF $\downarrow$	WER $\downarrow$	SIM $\uparrow$	NISQA $\uparrow$
GT	-	-	2.181	0.677 $\pm$ 0.006	4.070 $\pm$ 0.029
Ours	4	<b>0.006</b>	11.432	0.335 $\pm$ 0.003	2.623 $\pm$ 0.020
	8	<u>0.011</u>	2.818	<u>0.472</u> $\pm$ 0.003	3.916 $\pm$ 0.014
	16	0.019	<u>2.679</u>	<b>0.476</b> $\pm$ 0.003	3.994 $\pm$ 0.014
	32	0.037	<b>2.639</b>	<u>0.472</u> $\pm$ 0.003	4.033 $\pm$ 0.014
	64	0.071	2.705	0.470 $\pm$ 0.003	<u>4.060</u> $\pm$ 0.014
	128	0.140	2.693	0.468 $\pm$ 0.003	<b>4.070</b> $\pm$ 0.014

artifacts commonly found in non-autoregressive GAN vocoders. Furthermore, we measured the real-time factor (RTF) on an RTX 4090 GPU to quantify inference speed. Our evaluation is conducted using audio samples sourced from the test-clean and test-other subsets of LibriTTS<sup>3</sup>.

We report the results in Table 2. In terms of NISQA scores, the speech autoencoder performs competitively, achieving 4.06 on test-clean and outperforming BigVGAN on test-other with a score of 3.76. Similarly, in terms of UTMOSv2 scores, the speech autoencoder slightly lags behind BigVGAN on test-clean but surpasses it on test-other. This indicates that the speech autoencoder can synthesize perceptually high-quality speech. For the F1 evaluation of V/UV classification, BigVGAN achieves the highest scores (0.9735 on test-clean and 0.9620 on test-other), while the speech autoencoder follows closely with 0.9587 and 0.9450, respectively. This suggests that our model introduces minor artifacts affecting voiced/unvoiced classification. Nonetheless, the overall performance remains competitive considering the V/UV F1 scores of other neural vocoders reported in the baseline paper<sup>4</sup>. Notably, the speech autoencoder achieves an inference speed more than 20 times faster than BigVGAN. These results collectively confirm that the speech autoencoder, despite its bottlenecked architecture and low-dimensional latent space, can generate high-quality speech while offering significantly faster inference.

## 4.2 Trade-off between the number of function evaluations and synthesis quality

SupertonicTTS synthesizes speech through Euler’s method during inference. By adjusting the number of function evaluations (NFE), we can balance the trade-off between synthesis speed and quality. To quantify this relationship, we generated five samples per utterance from the test-clean subset of LibriSpeech [40] with varying NFE values and evaluated RTF, word error rate (WER), NISQA score [38], and speaker similarity (SIM). SIM was calculated as the cosine similarity between speaker embeddings from the generated speech and the corresponding 3-second reference, using the WavLM-TDNN model [7].

The evaluation results, presented in Table 3, demonstrate a general trend that increasing NFE leads to improvements in the WER, SIM, and NISQA scores. Specifically, the best scores for WER and SIM were obtained at NFE values of 32 and 16, respectively. This suggests that NFE values exceeding 32 effectively capture intelligibility, prosodic naturalness, and speaker identity. Meanwhile, NISQA scores exhibited a consistent positive correlation with NFE, suggesting that higher NFE values result

<sup>3</sup>In this study, all evaluations were conducted using audio samples ranging from 4 to 10 seconds in length.

<sup>4</sup>The authors of BigVGAN [10] reported that HiFi-GAN [29] and WaveFlow [42] achieved V/UV F1 scores of 0.9300 and 0.9410, respectively, on the dev subsets of LibriTTS.

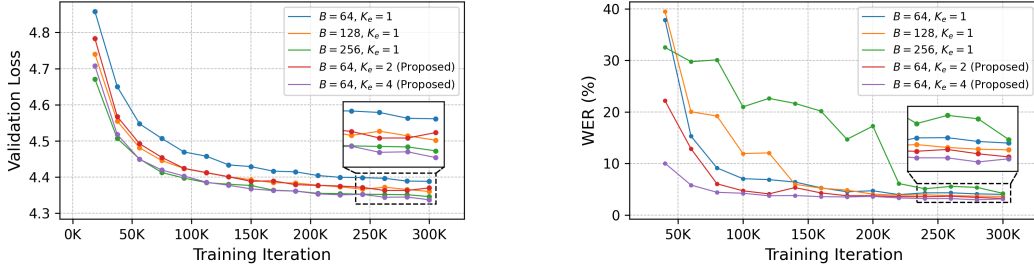


Figure 2: Comparison of the proposed batch expansion and increase in batch size. Validation losses (*left*) and WER results (*right*) are measured on the test-clean subsets of LibriTTS and LibriSpeech, respectively.

in enhanced audio fidelity. However, this improvement comes at the cost of increased processing time, as reflected in the RTF. Given this trade-off, we proceed with an NFE of 32 for further evaluations.

### 4.3 Evaluation of context-sharing batch expansion

To assess the impact of the context-sharing batch expansion on training efficiency, we trained four additional SupertonicTTS models using the following batch size ( $B$ ) and expansion factor ( $K_e$ ) combinations: (64, 1), (128, 1), (256, 1), and (64, 2). All other architectural and optimization settings remained unchanged. Performance was assessed using two metrics: validation loss and automatic speech recognition (ASR) results. Validation loss was computed on the test-clean subset of LibriTTS by averaging flow-matching losses (Eq. 1) across five timesteps: 0.1, 0.3, 0.5, 0.7, and 0.9. To ensure consistency, the reference mask  $\mathbf{m}$  was kept identical across all evaluations. For evaluation on ASR results, we generated five samples per utterance from the test-clean subset of LibriSpeech, using a 3-second reference speech segment cropped from a different utterance of the same speaker. For inference in the text-to-latent module, we used Euler’s method with 32 steps and a CFG coefficient of 3. The generated samples were transcribed using the CTC-based HuBERT-Large model<sup>5</sup> [15] and WER were calculated by comparing ground-truth transcriptions with ASR outputs. All transcriptions were normalized using NVIDIA’s NeMo-text-processing [57, 4] before measuring WER.

We present validation loss and WER curves throughout training up to 300k iterations in Figure 2. It can be observed that the validation loss converges faster as the expansion factor  $K_e$  increases. This trend is very similar to the effect of increasing the batch size  $B$ . Interestingly, we found that WER improves more quickly with an increase in the expansion factor, while increasing the batch size leads to degraded WER performance. We hypothesize that this is because the proposed method alleviates the speech-text alignment issue by using the same text and speech pair with different noise and time samples, and simply increasing the number of speech-text pairs does not effectively improve alignment learning. Evaluation results throughout the entire training process are provided in Appendix C.1.

We also assessed the computational efficiency of context-sharing batch expansion by analyzing memory usage, time per iteration, and the number of floating-point operations (GFLOPs). For testing, we used 15-second input speech, 250 characters, and 3-second reference speech. Iteration times were measured over 100 trials using a single RTX 4090 GPU, with 95% confidence intervals narrower than 0.2 ms. Table 4 presents the results for varying batch sizes  $B$  and expansion factors  $K_e$ . We observed that increasing  $K_e$  consistently offered better efficiency compared to increasing  $B$  across all metrics.

Table 4: GPU memory usage (GiB), iteration time (seconds), and GFLOPs across different batch sizes and expansion factors. GPU memory usage and iteration time were measured for a single training iteration, while GFLOPs were calculated from a single forward pass through the text-to-latent module.

$B$	$K_e$	Memory	Iter. Time	GFLOPs
16	1	2.47	0.083s	65.295
32	1	4.53	0.149s	130.59
16	2	<b>3.96</b>	<b>0.098s</b>	<b>120.07</b>
64	1	8.61	0.293s	261.18
16	4	<b>6.92</b>	<b>0.136s</b>	<b>229.63</b>

<sup>5</sup><https://huggingface.co/facebook/hubert-large-ls960-ft>.



Table 5: Performance comparison of SupertonicTTS with contemporary zero-shot TTS systems. Speaker similarity results, marked with and without a dagger ( $\dagger$ ), are measured using WavLM Base+ and WavLM-TDNN, respectively. “Inf. Time” represents the inference time required to generate a 10-second speech sample, and the specific GPU used for evaluation is reported when available. “Data” means the total amount of transcribed speech used for training. “#Param.” represents the total parameter count, including the vocoder and duration predictor. Best results are in bold, second-best are underlined.

	WER $\downarrow$	CER $\downarrow$	SIM $\uparrow$	Inf. Time $\downarrow$	Data (hour)	#Param.
GT	2.18	0.60	0.6770	-	-	-
VALL-E	5.9	-	-	$\sim$ 6.4s	60,000	410M
VoiceBox	<b>1.9</b>	-	<b>0.662</b>	$\sim$ 6.2s	60,000	371M
Mega-TTS 2	<u>2.46</u>	-	<u>0.898<math>\dagger</math></u>	3.02s (V100)	60,000	473M
CLaM-TTS	5.11	2.87	<u>0.495</u>	4.15s (A100)	55,000	>1.3B
DiTTo-TTS	2.56	<u>0.89</u>	<u>0.627</u>	<u>1.62s</u> (A100)	55,000	970M
Ours	2.64	<b>0.83</b>	0.472 / <b>0.915<math>\dagger</math></b>	<b>0.23s</b> (RTX 4090)	915	44M

Notably, raising  $K_e$  from 1 to 4 resulted in a 64% increase in iteration time, whereas increasing  $B$  by a factor of 4 led to a 253% increase. The overall results demonstrate that the proposed method improves training efficiency in memory usage and processing time by sharing conditional variables across batch data expanded from the same source.

#### 4.4 Comparison with other zero-shot TTS models

In this section, we benchmark our proposed model with state-of-the-art TTS systems. Specifically, we evaluate our model against five strong baselines: VALL-E [51], VoiceBox [30], Mega-TTS 2 [20], CLaM-TTS [25], and DiTTo-TTS [31]. These models exhibit impressive TTS performance, even in zero-shot scenarios. For the evaluation of SupertonicTTS, we followed the same experimental setup as described in Section 4.3: five samples were generated per utterance from the test-clean subset of LibriSpeech, using a 3-second reference speech from another utterance of the same speaker, with 32 inference steps and a CFG coefficient of 3. Additionally, we computed character error rates (CER) to assess the finer details of pronunciation in the synthesized speech. To compare speaker similarity with Mega-TTS 2, we also employed WavLM Base+<sup>6</sup> used in the Mega-TTS 2 paper. Inference time was measured by averaging the processing time for 100 generations of 10-second speech, performed on an RTX 4090.

Table 5 presents the evaluation results, with baseline scores sourced from their publications. In terms of WER, SupertonicTTS performed competitively with a score of 2.64, surpassing VALL-E (5.9) and CLaM-TTS (5.11). For CER, SupertonicTTS achieved a strong result of 0.83, outperforming DiTTo-TTS (0.89). These results suggest that SupertonicTTS can generate speech with minimal skipping, repetition, or mispronunciation issues. Regarding speaker similarity, as measured by WavLM-TDNN, SupertonicTTS scored 0.472 which is lower than VoiceBox (0.662), CLaM-TTS (0.495), and DiTTo-TTS (0.627). This difference may stem from SupertonicTTS’s lack of use of text information for reference speech unlike the other models, potentially affecting zero-shot performance. However, SupertonicTTS achieved a score of 0.915 when evaluated with WavLM Base+, surpassing Mega-TTS 2, which also does not use text for reference speech. Notably, these results were achieved with significantly fewer parameters and less than 2% of TTS dataset size compared to the baselines. Lastly, SupertonicTTS exhibited exceptional inference speed, requiring just 0.23 seconds to generate a 10-second speech sample. This result is considerably faster than the next fastest model, DiTTo-TTS, which requires 1.62 seconds. Overall, SupertonicTTS demonstrates competitive performance with remarkable efficiency in both architecture and training.

<sup>6</sup><https://huggingface.co/microsoft/wavlm-base-plus-sv>.

## 5 Conclusion

In this paper, we introduced SupertonicTTS, a novel text-to-speech system designed to effectively address the limitations of contemporary TTS models. By leveraging the LDM framework, we designed a system comprising a speech autoencoder, flow-matching-based text-to-latent module, and utterance-level duration predictor. To enhance scalability and efficiency, we incorporated a low-dimensional latent space, latent compression, context-sharing batch expansion, and ConvNeXt blocks. Furthermore, we simplified the pipeline by eliminating external dependencies such as G2P modules, text-speech aligners, and pretrained text encoders. Our extensive experiments validated that SupertonicTTS provides competitive zero-shot TTS performance with only 44 million parameters and fast inference speed. We believe the proposed system substantially reduces computational complexity and overhead in speech synthesis, opening promising avenues for future research in diverse speech applications and real-time scenarios.

## References

- [1] Junyi Ao, Rui Wang, Long Zhou, Chengyi Wang, Shuo Ren, Yu Wu, Shujie Liu, Tom Ko, Qing Li, Yu Zhang, Zihua Wei, Yao Qian, Jinyu Li, and Furu Wei. SpeechT5: Unified-modal encoder-decoder pre-training for spoken language processing. In *Proceedings of the 60th Annual Meeting of the Association for Computational Linguistics (Volume 1: Long Papers)*, pages 5723–5738, May 2022.
- [2] Kaito Baba, Wataru Nakata, Yuki Saito, and Hiroshi Saruwatari. The t05 system for the VoiceMOS Challenge 2024: Transfer learning from deep image classifier to naturalness MOS prediction of high-quality synthetic speech. In *IEEE Spoken Language Technology Workshop (SLT)*, 2024.
- [3] Evelina Bakhturina, Vitaly Lavrukhin, Boris Ginsburg, and Yang Zhang. Hi-Fi Multi-Speaker English TTS Dataset. *arXiv preprint arXiv:2104.01497*, 2021.
- [4] Evelina Bakhturina, Yang Zhang, and Boris Ginsburg. Shallow Fusion of Weighted Finite-State Transducer and Language Model for Text Normalization. In *Proc. Interspeech 2022*, 2022.
- [5] Edresson Casanova, Julian Weber, Christopher D Shulby, Arnaldo Candido Junior, Eren Gölge, and Moacir A Ponti. Yourtts: Towards zero-shot multi-speaker tts and zero-shot voice conversion for everyone. In *International Conference on Machine Learning*, pages 2709–2720. PMLR, 2022.
- [6] Edresson Casanova, Kelly Davis, Eren Gölge, Görkem Gökner, Iulian Gulea, Logan Hart, Aya Aljafari, Joshua Meyer, Reuben Morais, Samuel Olayemi, and Julian Weber. Xtts: a massively multilingual zero-shot text-to-speech model. *ArXiv*, abs/2406.04904, 2024. URL <https://api.semanticscholar.org/CorpusID:270357767>.
- [7] Sanyuan Chen, Chengyi Wang, Zhengyang Chen, Yu Wu, Shujie Liu, Zhuo Chen, Jinyu Li, Naoyuki Kanda, Takuya Yoshioka, Xiong Xiao, et al. Wavlm: Large-scale self-supervised pre-training for full stack speech processing. *IEEE Journal of Selected Topics in Signal Processing*, 16(6):1505–1518, 2022.
- [8] Hyeong-Seok Choi, Jinhyeok Yang, Juheon Lee, and Hyeongju Kim. Nansy++: Unified voice synthesis with neural analysis and synthesis. In *The Eleventh International Conference on Learning Representations*, 2023.
- [9] Tim Dettmers, Artidoro Pagnoni, Ari Holtzman, and Luke Zettlemoyer. Qlora: Efficient finetuning of quantized llms. *Advances in neural information processing systems*, 36:10088–10115, 2023.
- [10] Sang gil Lee, Wei Ping, Boris Ginsburg, Bryan Catanzaro, and Sungroh Yoon. BigVGAN: A universal neural vocoder with large-scale training. In *The Eleventh International Conference on Learning Representations*, 2023. URL [https://openreview.net/forum?id=iTtGCMDEzS\\_](https://openreview.net/forum?id=iTtGCMDEzS_).

- [11] Ian Goodfellow, Jean Pouget-Abadie, Mehdi Mirza, Bing Xu, David Warde-Farley, Sherjil Ozair, Aaron Courville, and Yoshua Bengio. Generative adversarial nets. *Advances in neural information processing systems*, 27, 2014.
- [12] Kaiming He, Xiangyu Zhang, Shaoqing Ren, and Jian Sun. Delving deep into rectifiers: Surpassing human-level performance on imagenet classification. In *Proceedings of the IEEE international conference on computer vision*, pages 1026–1034, 2015.
- [13] Jonathan Ho and Tim Salimans. Classifier-free diffusion guidance. In *NeurIPS 2021 Workshop on Deep Generative Models and Downstream Applications*, 2021. URL <https://openreview.net/forum?id=qw8AKxfYbI>.
- [14] Jonathan Ho, Ajay Jain, and Pieter Abbeel. Denoising diffusion probabilistic models. *Advances in neural information processing systems*, 33:6840–6851, 2020.
- [15] Wei-Ning Hsu, Benjamin Bolte, Yao-Hung Hubert Tsai, Kushal Lakhota, Ruslan Salakhutdinov, and Abdelrahman Mohamed. Hubert: Self-supervised speech representation learning by masked prediction of hidden units. *IEEE/ACM transactions on audio, speech, and language processing*, 29:3451–3460, 2021.
- [16] Sung-Feng Huang, Chyi-Jiunn Lin, Da-Rong Liu, Yi-Chen Chen, and Hung-yi Lee. Meta-tts: Meta-learning for few-shot speaker adaptive text-to-speech. *IEEE/ACM Transactions on Audio, Speech, and Language Processing*, 30:1558–1571, 2022.
- [17] Keith Ito and Linda Johnson. The lj speech dataset. <https://keithito.com/LJ-Speech-Dataset/>, 2017.
- [18] Won Jang, Daniel Chung Yong Lim, Jaesam Yoon, Bongwan Kim, and Juntae Kim. Univnet: A neural vocoder with multi-resolution spectrogram discriminators for high-fidelity waveform generation. In *Interspeech*, 2021. URL <https://api.semanticscholar.org/CorpusID:235435945>.
- [19] Myeonghun Jeong, Hyeongju Kim, Sung Jun Cheon, Byoung Jin Choi, and Nam Soo Kim. Diff-tts: A denoising diffusion model for text-to-speech. In *Interspeech*, 2021. URL <https://api.semanticscholar.org/CorpusID:233025015>.
- [20] Ziyue Jiang, Jinglin Liu, Yi Ren, Jinzheng He, Zhenhui Ye, Shengpeng Ji, Qian Yang, Chen Zhang, Pengfei Wei, Chunfeng Wang, Xiang Yin, Zejun MA, and Zhou Zhao. Mega-TTS 2: Boosting prompting mechanisms for zero-shot speech synthesis. In *The Twelfth International Conference on Learning Representations*, 2024. URL <https://openreview.net/forum?id=mvMI3N4AvD>.
- [21] Zeqian Ju, Yuancheng Wang, Kai Shen, Xu Tan, Detai Xin, Dongchao Yang, Yanqing Liu, Yichong Leng, Kaitao Song, Siliang Tang, et al. Naturalspeech 3: zero-shot speech synthesis with factorized codec and diffusion models. In *Proceedings of the 41st International Conference on Machine Learning*, pages 22605–22623, 2024.
- [22] Eugene Kharitonov, Damien Vincent, Zalán Borsos, Raphaël Marinier, Sertan Girgin, Olivier Pietquin, Matt Sharifi, Marco Tagliasacchi, and Neil Zeghidour. Speak, read and prompt: High-fidelity text-to-speech with minimal supervision. *Transactions of the Association for Computational Linguistics*, 11:1703–1718, 2023.
- [23] Jaehyeon Kim, Sungwon Kim, Jungil Kong, and Sungroh Yoon. Glow-tts: A generative flow for text-to-speech via monotonic alignment search. *Advances in Neural Information Processing Systems*, 33:8067–8077, 2020.
- [24] Jaehyeon Kim, Jungil Kong, and Juhee Son. Conditional variational autoencoder with adversarial learning for end-to-end text-to-speech. In *International Conference on Machine Learning*, pages 5530–5540. PMLR, 2021.
- [25] Jaehyeon Kim, Keon Lee, Seungjun Chung, and Jaewoong Cho. CLam-TTS: Improving neural codec language model for zero-shot text-to-speech. In *The Twelfth International Conference on Learning Representations*, 2024. URL <https://openreview.net/forum?id=ofzeypWosV>.

- [26] Jong Wook Kim, Justin Salamon, Peter Li, and Juan Pablo Bello. Crepe: A convolutional representation for pitch estimation. In *2018 IEEE international conference on acoustics, speech and signal processing (ICASSP)*, pages 161–165. IEEE, 2018.
- [27] Sungwon Kim, Heeseung Kim, and Sungroh Yoon. Guided-tts 2: A diffusion model for high-quality adaptive text-to-speech with untranscribed data. *arXiv preprint arXiv:2205.15370*, 2022.
- [28] Sungwon Kim, Kevin Shih, Joao Felipe Santos, Evelina Bakhturina, Mikyas Desta, Rafael Valle, Sungroh Yoon, Bryan Catanzaro, et al. P-flow: a fast and data-efficient zero-shot tts through speech prompting. *Advances in Neural Information Processing Systems*, 36, 2024.
- [29] Jungil Kong, Jaehyeon Kim, and Jaekyoung Bae. Hifi-gan: Generative adversarial networks for efficient and high fidelity speech synthesis. *Advances in neural information processing systems*, 33:17022–17033, 2020.
- [30] Matthew Le, Apoorv Vyas, Bowen Shi, Brian Karrer, Leda Sari, Rashed Moritz, Mary Williamson, Vimal Manohar, Yossi Adi, Jay Mahadeokar, et al. Voicebox: Text-guided multilingual universal speech generation at scale. *Advances in neural information processing systems*, 36, 2024.
- [31] Keon Lee, Dong Won Kim, Jaehyeon Kim, Seungjun Chung, and Jaewoong Cho. DiTTo-TTS: Diffusion transformers for scalable text-to-speech without domain-specific factors. In *The Thirteenth International Conference on Learning Representations*, 2025. URL <https://openreview.net/forum?id=hQvX9MBowC>.
- [32] Yaron Lipman, Ricky T. Q. Chen, Heli Ben-Hamu, Maximilian Nickel, and Matthew Le. Flow matching for generative modeling. In *The Eleventh International Conference on Learning Representations*, 2023. URL <https://openreview.net/forum?id=PqvMRDCJT9t>.
- [33] Aixin Liu, Bei Feng, Bin Wang, Bingxuan Wang, Bo Liu, Chenggang Zhao, Chengqi Deng, Chong Ruan, Damai Dai, Daya Guo, et al. Deepseek-v2: A strong, economical, and efficient mixture-of-experts language model. *arXiv preprint arXiv:2405.04434*, 2024.
- [34] Zhuang Liu, Hanzi Mao, Chao-Yuan Wu, Christoph Feichtenhofer, Trevor Darrell, and Saining Xie. A convnet for the 2020s. *Proceedings of the IEEE/CVF Conference on Computer Vision and Pattern Recognition (CVPR)*, 2022.
- [35] Ilya Loshchilov and Frank Hutter. Decoupled weight decay regularization. In *International Conference on Learning Representations*, 2019. URL <https://openreview.net/forum?id=Bkg6RiCqY7>.
- [36] Justin Lovelace, Varsha Kishore, Chao Wan, Eliot Shekhtman, and Kilian Q Weinberger. Latent diffusion for language generation. *Advances in Neural Information Processing Systems*, 36: 56998–57025, 2023.
- [37] Justin Lovelace, Soham Ray, Kwangyoun Kim, Kilian Q Weinberger, and Felix Wu. Simple-TTS: End-to-end text-to-speech synthesis with latent diffusion, 2024. URL <https://openreview.net/forum?id=m4mwbPj0wb>.
- [38] Gabriel Mittag, Babak Naderi, Assmaa Chehadi, and Sebastian Möller. Nisqa: A deep cnn-self-attention model for multidimensional speech quality prediction with crowdsourced datasets. In *Interspeech*, 2021. URL <https://api.semanticscholar.org/CorpusID:233296150>.
- [39] Takuma Okamoto, Haruki Yamashita, Yamato Ohtani, Tomoki Toda, and Hisashi Kawai. Wavenext: Convnext-based fast neural vocoder without istft layer. In *2023 IEEE Automatic Speech Recognition and Understanding Workshop (ASRU)*, pages 1–8. IEEE, 2023.
- [40] Vassil Panayotov, Guoguo Chen, Daniel Povey, and Sanjeev Khudanpur. Librispeech: An asr corpus based on public domain audio books. In *2015 IEEE International Conference on Acoustics, Speech and Signal Processing (ICASSP)*, pages 5206–5210, 2015. doi: 10.1109/ICASSP.2015.7178964.

- [41] Puyuan Peng, Shang-Wen Li, Po-Yao Huang, Abdelrahman Mohamed, and David Harwath. Voicecraft: Zero-shot speech editing and text-to-speech in the wild. *ACL*, 2024.
- [42] Wei Ping, Kainan Peng, Kexin Zhao, and Zhao Song. Waveflow: A compact flow-based model for raw audio. In *International Conference on Machine Learning*, pages 7706–7716. PMLR, 2020.
- [43] Dustin Podell, Zion English, Kyle Lacey, Andreas Blattmann, Tim Dockhorn, Jonas Müller, Joe Penna, and Robin Rombach. SDXL: Improving latent diffusion models for high-resolution image synthesis. In *The Twelfth International Conference on Learning Representations*, 2024. URL <https://openreview.net/forum?id=di52zR8xgf>.
- [44] Vadim Popov, Ivan Vovk, Vladimir Gogoryan, Tasnima Sadekova, and Mikhail Kudinov. Grad-tts: A diffusion probabilistic model for text-to-speech. In *International Conference on Machine Learning*, pages 8599–8608. PMLR, 2021.
- [45] Robin Rombach, Andreas Blattmann, Dominik Lorenz, Patrick Esser, and Björn Ommer. High-resolution image synthesis with latent diffusion models. In *Proceedings of the IEEE/CVF conference on computer vision and pattern recognition*, pages 10684–10695, 2022.
- [46] Takaaki Saeki, Soumi Maiti, Xinjian Li, Shinji Watanabe, Shinnosuke Takamichi, and Hiroshi Saruwatari. Learning to speak from text: Zero-shot multilingual text-to-speech with unsupervised text pretraining. In Edith Elkind, editor, *Proceedings of the Thirty-Second International Joint Conference on Artificial Intelligence, IJCAI-23*, pages 5179–5187. International Joint Conferences on Artificial Intelligence Organization, 8 2023. doi: 10.24963/ijcai.2023/575. URL <https://doi.org/10.24963/ijcai.2023/575>. Main Track.
- [47] Hubert Siuzdak. Vocos: Closing the gap between time-domain and fourier-based neural vocoders for high-quality audio synthesis. In *The Twelfth International Conference on Learning Representations*, 2024. URL <https://openreview.net/forum?id=vY9nzQmQBw>.
- [48] Yang Song, Jascha Sohl-Dickstein, Diederik P Kingma, Abhishek Kumar, Stefano Ermon, and Ben Poole. Score-based generative modeling through stochastic differential equations. *arXiv preprint arXiv:2011.13456*, 2020.
- [49] Jaesung Tae, Hyeongju Kim, and Taesu Kim. Editts: Score-based editing for controllable text-to-speech. In *Interspeech*, 2021. URL <https://api.semanticscholar.org/CorpusID:238408421>.
- [50] Ashish Vaswani, Noam Shazeer, Niki Parmar, Jakob Uszkoreit, Llion Jones, Aidan N Gomez, Łukasz Kaiser, and Illia Polosukhin. Attention is all you need. In I. Guyon, U. Von Luxburg, S. Bengio, H. Wallach, R. Fergus, S. Vishwanathan, and R. Garnett, editors, *Advances in Neural Information Processing Systems*, volume 30. Curran Associates, Inc., 2017. URL [https://proceedings.neurips.cc/paper\\_files/paper/2017/file/3f5ee243547dee91fbd053c1c4a845aa-Paper.pdf](https://proceedings.neurips.cc/paper_files/paper/2017/file/3f5ee243547dee91fbd053c1c4a845aa-Paper.pdf).
- [51] Chengyi Wang, Sanyuan Chen, Yu Wu, Zi-Hua Zhang, Long Zhou, Shujie Liu, Zhuo Chen, Yanqing Liu, Huaming Wang, Jinyu Li, Lei He, Sheng Zhao, and Furu Wei. Neural codec language models are zero-shot text to speech synthesizers. *IEEE Transactions on Audio, Speech and Language Processing*, 33:705–718, 2023. URL <https://api.semanticscholar.org/CorpusID:255440307>.
- [52] Xinsheng Wang, Mingqi Jiang, Ziyang Ma, Ziyu Zhang, Songxiang Liu, Linqin Li, Zheng Liang, Qixi Zheng, Rui Wang, Xiaoqin Feng, et al. Spark-tts: An efficient llm-based text-to-speech model with single-stream decoupled speech tokens. *arXiv preprint arXiv:2503.01710*, 2025.
- [53] Linting Xue, Aditya Barua, Noah Constant, Rami Al-Rfou, Sharan Narang, Mihir Kale, Adam Roberts, and Colin Raffel. Byt5: Towards a token-free future with pre-trained byte-to-byte models. *Transactions of the Association for Computational Linguistics*, 10:291–306, 2022.
- [54] Junichi Yamagishi, Christophe Veaux, and Kirsten MacDonald. CSTR VCTK Corpus: English multi-speaker corpus for CSTR voice cloning toolkit (version 0.92), 2019.

- [55] Jinhyeok Yang, Junhyeok Lee, Hyeong-Seok Choi, Seunghoon Ji, Hyeongju Kim, and Juheon Lee. Dualspeech: Enhancing speaker-fidelity and text-intelligibility through dual classifier-free guidance. In *Proc. Interspeech 2024*, pages 4423–4427, 2024.
- [56] Heiga Zen, Viet Dang, Rob Clark, Yu Zhang, Ron J Weiss, Ye Jia, Zhifeng Chen, and Yonghui Wu. Libritts: A corpus derived from librispeech for text-to-speech. *arXiv preprint arXiv:1904.02882*, 2019.
- [57] Yang Zhang, Evelina Bakhturina, and Boris Ginsburg. NeMo (Inverse) Text Normalization: From Development to Production. In *Proc. Interspeech 2021*, pages 4857–4859, 2021.

## A Architecture details

### A.1 Speech autoencoder

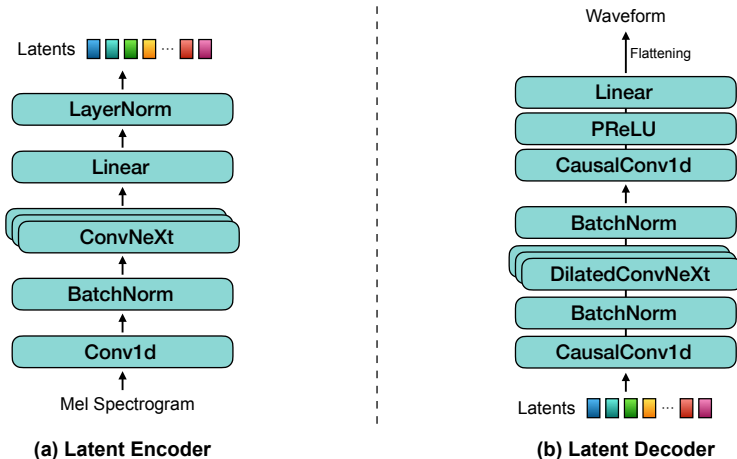


Figure 3: Detailed architecture of latent encoder and latent decoder in speech autoencoder.

We illustrate the detailed architecture of the speech autoencoder in Figure 3. Both the latent encoder and the latent decoder are built on the Vocos architecture [47] with several modifications, aiming for useful applications (e.g., latent encoding, fast inference, and low-latency TTS).

#### A.1.1 Latent encoder

The first convolutional layer of the latent encoder, followed by batch normalization, transforms a 228-dimensional mel spectrogram into hidden representations, preserving the sequence length and expanding the dimensionality to 512. The latent encoder employs 10 ConvNeXt blocks, with an intermediate dimension of 2048. The intermediate dimension refers to the hidden size between two consecutive  $1 \times 1$  convolutional layers within each ConvNeXt block. A final linear layer, followed by layer normalization, projects the 512-dimensional output of the ConvNeXt blocks into a 24-dimensional latent space. All convolutional layers in the latent encoder use a kernel size of 7. In summary, the latent encoder compresses a 228-dimensional mel spectrogram into 24-dimensional latents while maintaining the original sequence length.

#### A.1.2 Latent decoder

The latent decoder begins with a convolutional layer followed by batch normalization, transforming the 24-dimensional latents into hidden representations of size 512. It then processes these representations through 10 dilated ConvNeXt blocks, each with an intermediate dimension of 2048, followed by another batch normalization. The depthwise convolutional layers within these blocks use dilation rates of  $[1, 2, 4, 1, 2, 4, 1, 1, 1, 1]$ . Next, a convolutional layer with a kernel size of 3 converts the normalized output of the ConvNeXt blocks to hidden representations of dimension 2048. A final linear layer then projects these representations into frame-level outputs with 512 channels. These outputs are subsequently reshaped into a single-channel format, producing the final waveform output. The first convolutional layer and the depthwise convolutional layers within each ConvNeXt block use a kernel size of 7. Additionally, all convolutional layers in the latent decoder operate in a causal manner.

#### A.1.3 Discriminator

We adopt a lightweight version of multi-period discriminators (MPDs) introduced in HiFi-GAN [29]. Each MPD consists of six convolutional layers with hidden sizes 16, 64, 256, 512, 512, and 1. The period settings remain the same as the original configuration: 2, 3, 5, 7, and 11. For multi-resolution discriminators (MRDs), log-scaled linear spectrograms serve as input, with three different FFT sizes: 512, 1024, and 2048. The hop sizes are set to one-quarter of the corresponding FFT size, while the

Table 6: Configuration of convolutional layers in multi resolution discriminator.

Layer	Input Channels	Output Channels	Kernel Size	Stride
Conv2D	1	16	(5, 5)	(1, 1)
Conv2D	16	16	(5, 5)	(2, 1)
Conv2D	16	16	(5, 5)	(2, 1)
Conv2D	16	16	(5, 5)	(2, 1)
Conv2D	16	16	(5, 5)	(1, 1)
Conv2D	16	1	(3, 3)	(1, 1)

window sizes equal to the FFT sizes. We use the Hann window function for spectral analysis. Each MRD consists of six convolutional layers, as detailed in Table 6.

## A.2 Text-to-latent module

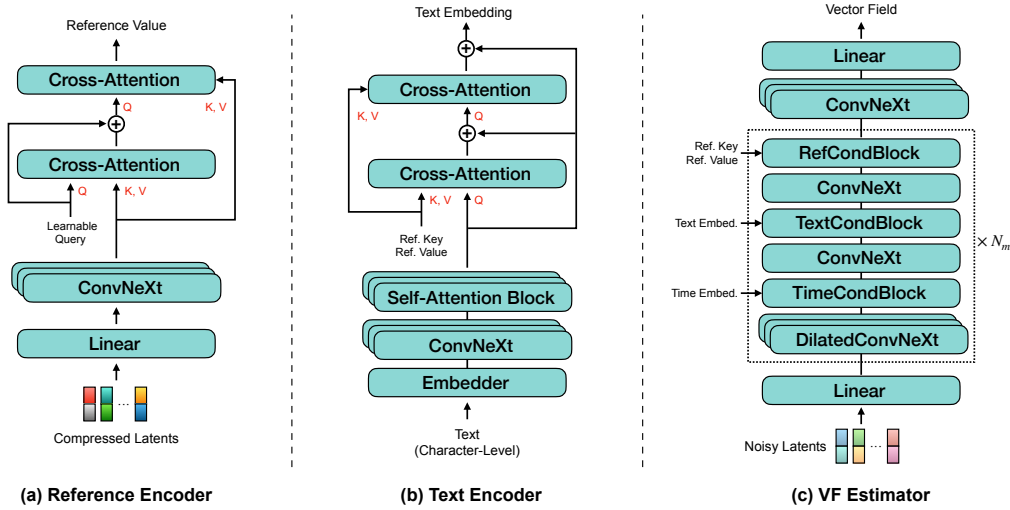


Figure 4: Detailed architecture of reference encoder, text encoder, and VF estimator in text-to-latent module. Q, K, and V represent the inputs used to compute query, key, and value, respectively, in attention mechanism.

We illustrate the detailed architecture of the text-to-latent module in Figure 4. Each component is carefully designed to operate efficiently with a simple architecture. Note that the text-to-latent module does not rely on any external pretrained models, G2P modules, or text-speech aligners.

### A.2.1 Reference encoder

The reference encoder is composed of a linear layer, 6 ConvNeXt blocks, and 2 cross-attention layers. The linear layer transforms temporally compressed latents with a dimension of 144 to hidden representations with a dimension of 128. The kernel size and intermediate dimension of all ConvNeXt blocks are set to 5 and 512, respectively. In the cross-attention layers, three linear layers with the same input and output dimensions are used to generate query, key, and value. To obtain a fixed number of vectors (i.e., the reference value shown in Figure 4 (a)) representing reference speech, 50 learnable vectors with a dimension of 128 are used in the first attention block.

### A.2.2 Text encoder

The text encoder consists of an embedder, 6 ConvNeXt blocks, 4 self-attention blocks, and 2 cross-attention layers. The embedder maps each character to a 128-dimensional vector with a simple lookup table. The kernel size and intermediate dimension of ConvNeXt blocks are set to 5 and 512, respectively. The self-attention blocks follow the transformer encoder architecture, configured with 512 filter channels, 4 attention heads, and rotary position embedding. The cross-attention layers



consist of three linear layers with same input and output dimensions, and the first cross-attention layer utilizes 50 learnable vectors (i.e., the reference key shown in Figure 4 (b)), each with a dimension of 128. These 50 vectors are reused as keys in the VF estimator.

### A.2.3 VF estimator

The first linear layer in the VF estimator maps 144-dimensional noisy latents to 256-dimensional hidden representations. The main block, highlighted with dotted lines in Figure 4 (c), is composed of 4 dilated ConvNeXt blocks, 2 standard ConvNeXt blocks, TimeCondBlock, TextCondBlock, and RefCondBlock. Each ConvNeXt block has a kernel size of 5 and an intermediate dimension of 1024. The dilation rates for the four dilated ConvNeXt blocks are set to 1, 2, 4, and 8, respectively. TimeCondBlock employs a single linear layer to project a 64-dimensional time embedding onto the channel dimension of input and performs time conditioning via global addition. The time embedding is computed using the same method as in Grad-TTS [44]. TextCondBlock and RefCondBlock employ a cross-attention mechanism to incorporate text and reference speech information, respectively. This structure is repeated four times ( $N_m = 4$ ). Finally, 4 additional ConvNeXt blocks are applied, followed by a linear layer that maps the 256-dimensional representation back to a 144-dimensional output.

## A.3 Duration predictor

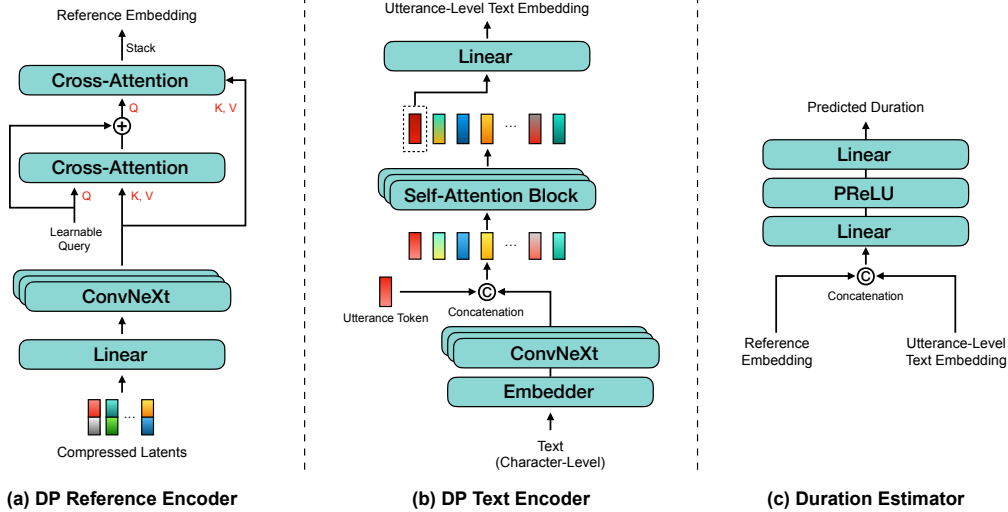


Figure 5: Detailed architecture of DP reference encoder, DP text encoder, and duration estimator in duration predictor.

We illustrate the detailed architecture of the duration predictor in Figure 5. Since predicting total duration is simpler than phoneme-level duration prediction, we designed this module to be lightweight. Notably, it contains only about 0.5 million parameters.

### A.3.1 DP reference encoder

The DP reference encoder shares the same architecture as the reference encoder in the text-to-latent module but with different hyperparameter settings. It consists of a linear layer, 4 ConvNeXt blocks, and 2 cross-attention layers. The initial linear layer maps a 144-dimensional input to a 64-dimensional representation. Each ConvNeXt block has a kernel size of 5 and an intermediate dimension of 256. The cross-attention layers project inputs into 16-dimensional vectors and apply the attention mechanism. In the first cross-attention layer, queries are computed using eight learnable vectors. The final reference embedding is obtained by stacking the outputs along the channel dimension, resulting in a 64-dimensional vector.

### A.3.2 DP text encoder

The DP text encoder comprises an embedder, 6 ConvNeXt blocks, 2 self-attention blocks, and a linear layer. The embedder converts character-level text input into 64-dimensional vectors. The kernel size and intermediate dimension of each ConvNeXt block are set to 5 and 256, respectively. A learnable 64-dimensional vector, referred to as the utterance token in Figure 5 (b), is prepended to the output of the ConvNeXt blocks. The self-attention blocks have 256 filter channels, 2 attention heads, and incorporate rotary position embeddings. Finally, the first vector from the output of the last self-attention block passes through a linear layer with the same input and output dimension, producing an utterance-level text embedding.

### A.3.3 Duration estimator

The duration estimator consists of two linear layers with a PReLU activation. The first layer maintains the input and output dimensions at 164, while the second layer maps the output to a single scalar value. The outputs from the DP reference encoder and the DP text encoder are concatenated before being passing to the first linear layer, as shown in Figure 5 (c).

## B Optimization details

### B.1 Speech autoencoder

The training of the speech autoencoder is conducted within the framework of a Generative Adversarial Network (GAN) [11]. The two primary training objectives for the generator and discriminators are as follows:

$$\mathcal{L}_G = \lambda_{\text{recon}}\mathcal{L}_{\text{recon}}(G) + \lambda_{\text{adv}}\mathcal{L}_{\text{adv}}(G; D) + \lambda_{\text{fm}}\mathcal{L}_{\text{fm}}(G; D), \quad (2)$$

$$\mathcal{L}_D = \mathcal{L}_{\text{adv}}(D; G), \quad (3)$$

where  $G$  represents the generator,  $D$  denotes the composite of discriminators. The reconstruction loss,  $\mathcal{L}_{\text{recon}}$ , is computed using a spectral  $L_1$  loss over multi-resolution mel spectrograms. Specifically, three separate mel spectrograms are generated using different FFT sizes: 1024, 2048, and 4096. These spectrograms are paired with corresponding mel band counts of 64, 128, and 128, respectively. Hop sizes are set to one-quarter of the corresponding FFT sizes. A Hann window is applied to each spectrogram, with the window size matching the respective FFT size used for that spectrogram. The adversarial losses,  $\mathcal{L}_{\text{adv}}$ , are computed as follows:

$$\mathcal{L}_{\text{adv}}(G; D) = \mathbb{E}_{x \sim p(x)} [(D(G(x)) - 1)^2], \quad (4)$$

$$\mathcal{L}_{\text{adv}}(D; G) = \mathbb{E}_{x \sim p(x)} [(D(G(x)) + 1)^2 + (D(x) - 1)^2], \quad (5)$$

where  $x$  denotes the ground truth audio and  $G(x)$  represents the reconstructed audio. The feature matching loss,  $\mathcal{L}_{\text{fm}}$ , is obtained by averaging the  $L_1$  distances between intermediate features of each discriminator layer, derived from both real and generated speech:

$$\mathcal{L}_{\text{fm}}(G; D) = \frac{1}{L} \sum_{l=1}^L \|\phi_l(G(x)) - \phi_l(x)\|_1, \quad (6)$$

where  $L$  denotes the total number of layers in the discriminators and  $\phi_l(\cdot)$  refers to the feature representations obtained from the  $l$ -th discriminator layer.

## C Additional experimental results

### C.1 Experimental results on evaluation of context-sharing batch expansion

Figure 6 presents validation loss and ASR results throughout the entire training process. Increasing the expansion factor  $K_e$  consistently accelerates convergence for both validation loss and WER. In

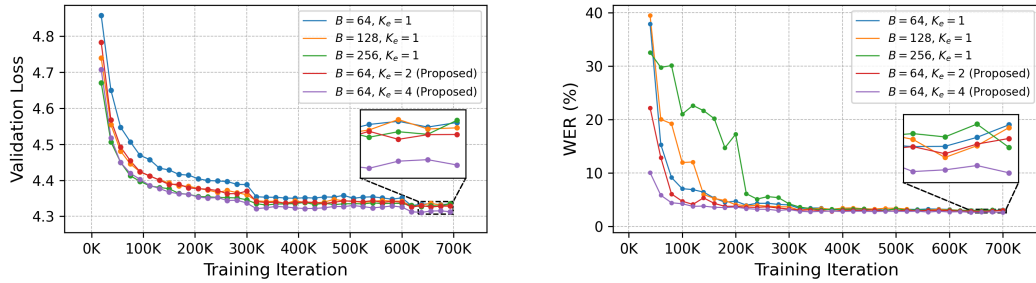


Figure 6: Model performance tracked throughout the entire training process. Validation losses (*left*) and WER results (*right*) are measured on the test-clean subsets of LibriTTS and LibriSpeech, respectively.

contrast, while increasing the batch size  $B$  helps reduce validation loss, it slows the convergence of WER. This indicates that simply increasing the batch size is not sufficient for achieving accurate text-speech alignment. Additionally, this experiment demonstrates that the proposed batch expansion algorithm not only accelerates loss convergence but also alleviates issues such as word skipping, repetition, and mispronunciation.